applied optics

Field diversity phase retrieval method for wavefront sensing in monolithic mirror space telescopes

Guohao Ju,[1,2,*] Changxiang Yan,[1] Dan Yue,[3] and Zhiyuan Gu[1]

[1]Changchun Institute of Optics, Fine Mechanics and Physics, Chinese Academy of Sciences, Changchun 130033, China
[2]University of Chinese Academy of Sciences, Beijing 100049, China
[3]School of Optoelectronic Engineering, Changchun University of Science and Technology, Changchun 130022, China
*Corresponding author: juguohao123@163.com

Received 23 February 2017; revised 12 April 2017; accepted 12 April 2017; posted 12 April 2017 (Doc. ID 287386); published 11 May 2017

To guarantee the uniqueness of the solution for the wavefront phase, a series of intensity images with known phase diversities is usually needed in the current phase retrieval wavefront sensing methods. However, to obtain these intensity images with deliberately added diversity phases, some additional instruments (e.g., beam splitters) or operations (e.g., adjustment of the focus) are usually needed, which can pose a challenge for wavefront sensing in space telescopes. This paper proposes a new concept for retrieving the wavefront phase of monolithic mirror space telescopes with perturbations, where the intensity measurements with phase diversities are directly obtained from different field positions of one image, without the need for any additional instruments or operations. To realize this new concept, we present a modified phase diversity method to account for the unknown phase diversities between these intensity measurements based on an in-depth understanding of the net aberration fields induced by misalignments and figure errors. Relevant simulations for different cases are performed to demonstrate the feasibility and accuracy of the proposed method. Since in this method the phase diversities between different intensity measurements are mainly induced by the diversities in the field position, we call it the field diversity phase retrieval method. This work can present great facility for wavefront sensing in monolithic mirror space telescopes.

OCIS codes: (010.7350) Wave-front sensing; (100.5070) Phase retrieval; (110.6770) Telescopes; (220.1080) Active or adaptive optics.

https://doi.org/10.1364/AO.56.004224

1. INTRODUCTION

Due to complete freedom from atmospheric turbulence effects, space-based telescopes can achieve sharper images than the ground-based ones (even with adaptive optical systems) [1]. However, they can still suffer from their own fixed or quasi-static internal aberrations. These aberrations can originate from various thermal/mechanical stresses on the optics or errors in the fabrication of the optical system. Active optics systems present an efficient solution to this problem, which can correct these aberrations during observing periods [2]. Key to these corrections has been accurate measurement of the wavefront.

Phase retrieval wavefront sensing (WFS) represents a class of image-based WFS methods that utilize intensity measurements to recover the wavefront phase of optical systems. Presently, phase retrieval methods can be classified into two general categories [3,4]: iterative-transform and parametric methods. The former, which is also known as the Gerchberg–Saxton or error-reduction algorithm, involves iterative Fourier transformation back and forth between the object and Fourier domains and application of the measured data or known constraints in each domain [5,6]. The latter, which is also known as the model-based optimization algorithm or directly called the phase diversity algorithm, recovers the parameterized wavefront aberrations by minimizing the optimization objective function (error metric) with nonlinear optimization methods [7–10]. Both of these two classes of phase retrieval algorithms have played an important role in estimating the wavefront aberrations of large astronomical telescopes [11–16].

Note that the mathematical mapping from the set of all possible pupil phase screens to the set of all possible intensity distributions is a many-to-one mapping. Therefore, to invert this mapping and guarantee the uniqueness of the solution for the wavefront phase, the phase retrieval algorithms mentioned above (especially the second class) usually require a simultaneous collection of multiple intensity images with certain phase diversities. In principle, any form of known phase diversity can serve as the diversity function. However, compared to other forms of diversity, such as wavelength diversity [17],

illumination diversity [18], subaperture piston diversity [19], transverse translation diversity [20–22], and generalized phase diversity [23], defocus diversity is usually simpler to implement in practice and therefore is the most widely used form of phase diversity.

However, to obtain a pair of intensity images with defocus diversity, we still need some additional instruments or operations. These additional instruments and operations can pose a challenge for wavefront sensing in space telescopes. Specifically, a beam splitter and an additional detector are usually needed if we want to obtain a pair of intensity images with defocus diversity simultaneously. However, taking into account the fact that spaceborne systems operate in a hostile, inacceptable environment, and the systems designers face significant cost, size, and weight constraints, it is unpractical to apply beam splitters to wavefront sensing in space telescopes. If beam splitters are not available, we need to translate the image plane to deliberately introduce defocus diversity. However, this can increase uncertainty and decrease the efficiency for wavefront sensing in space telescopes. Besides, the pair of intensity measurements with defocus diversity is not obtained simultaneously in this case. It is possible that the aberration condition of the system changes during this process, which can definitely introduce error in the recovered wavefront phase.

To achieve the goal of reconstructing the wavefront of the system without any additional hardware or operation and greatly increase the efficiency, this paper first presents a new concept for wavefront sensing in space telescopes. Specifically, we propose that a series of intensity measurements obtained from different field positions of one image can be used to retrieve the wavefront of the system. Importantly, the phase diversities between different intensity measurements are unknown in this case. We then realize this concept for monolithic mirror space telescopes by presenting a modified phase diversity phase retrieval method based on an in-depth understanding of the aberration field characteristics of the monolithic mirror space telescopes in the nominal or perturbed state. In this method, the emphasis is no longer on the aberration coefficients for a specific field point but on the field dependencies of different aberration types over the whole field. The wavefront aberrations for different field points can be retrieved simultaneously. Detailed simulations for different cases are performed to demonstrate the feasibility and accuracy of the proposed method. This work can bring great facility for wavefront sensing in space telescopes with a monolithic primary mirror.

This paper is organized as follows. In Section 2, we present a new concept for phase retrieval wavefront sensing in space telescopes. Then we continue to realize this concept for monolithic mirror space telescopes in Section 3 by proposing a modified phase diversity algorithm. In Section 4, we present detailed simulations for different cases to demonstrate the feasibility and accuracy of the proposed method. We summarize and conclude the paper in Section 5.

2. NEW CONCEPT FOR PHASE RETRIEVAL WAVEFRONT SENSING IN SPACE TELESCOPES

As mentioned in the previous section, a series of intensity measurements with phase diversity is usually needed in phase retrieval algorithms to guarantee the uniqueness of the solution. On the other hand, we also showed that while defocus diversity is usually selected as the diversity function in practice due to its simplicity for implementation, some additional instruments (e.g., beam splitters) or operations (e.g., adjustment of the focus) are still needed, which can pose a challenge for wavefront sensing in space telescopes. In this section, we first rediscuss the challenges posed by the additional instruments and operations that are needed to obtain a pair of intensity measurements with defocus diversity. Then we propose a new concept for wavefront sensing in space telescopes, where a series of intensity measurements with phase diversity can be obtained simultaneously without the need for any additional instruments and operations. Several specific forms for the setting of the wavefront sensors relevant to this wavefront sensing concept are also presented.

A. Challenges in Defocus Diversity Phase Retrieval for Space Telescopes

Defocus diversity is the most common phase diversity used for phase retrieval wavefront sensing, especially for space telescopes. However, some additional instruments and operations are still needed, which can pose a challenge for space telescopes. We will further discuss this problem in this section.

To obtain a pair of intensity measurements with defocus diversity simultaneously, beam splitters are usually needed. There are two kinds of beam splitters, i.e., plate beam splitters and cube beam splitters, as shown in Fig. 1. The main problems of the plate beam splitter are presented below:

(1) Plate beam splitters are not stable and compact enough for space usage. Besides, they are hard to mount and align. Therefore, they not only decrease the stability and increase the risk of the system but also increase the difficulties in engineering implementation and the cost.

(2) The path lengths for the reflected and the transmitted beams are not identical. The plate beam splitters can introduce a large astigmatism when they are placed in a convergent beam, especially with a large incident angle, as shown in Fig. 1(a). Therefore, the additional aberrations introduced by beam splitters must be carefully calibrated. Besides, this also increases the requirement for the range of the aberrations that can be recovered.

Cube beam splitters seem better, considering the two problems of plate beam splitters presented above. However, cube beam splitters are usually heavier and larger than plate beam splitters. Note that wavefront sensing at multiple field points is usually needed to determine the perturbation state of the system, which indicates that several beam splitters are needed (wavefront sensing at one field point needs a beam splitter). Therefore, cube beam splitters can greatly increase the weight and size of the system.

Besides, there are other common problems for these two kinds of beam splitters. For example, spaceborne systems operate in a hostile and inacceptable environment, so we need to consider whether the optical properties of the beam splitters will remain unchanged on orbit. Additional detectors are also needed, which will further increase the weight and size of the system. Errors in fabricating and mounting of these beam splitters can also exist, so we need to do some additional calibration

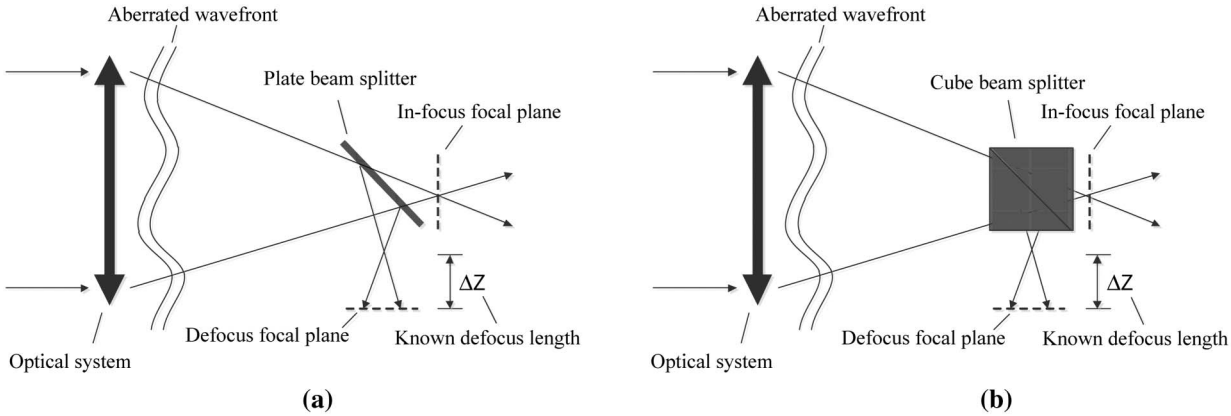

Fig. 1. Schematics for defocus diversity phase retrieval wavefront sensing with two kinds of beam splitters: (a) a plate beam splitter and (b) a cube beam splitter.

work to account for these error. Therefore, beam splitters are very unsuitable for wavefront sensing in space telescopes.

There is another method to obtain a pair of intensity measurements with defocus diversity. We can first obtain an in-focus intensity image, and then we obtain a defocus intensity image after translating the image plane to deliberately introduce defocus diversity. In this case, no additional instruments are needed. However, one additional operation, i.e., translation of the image plane is needed. This additional operation can increase the uncertainty of the system, because the system is further perturbed in this process. The efficiency of the wavefront sensing process is also decreased, because the adjustment of the focus can take some time and if wavefront measurements at several field points are needed, we needed to repeat this process several times. Another important problem of this method is that the two measurements are obtained at different times. Space telescopes travel on their specific obits all the time. The stress state of the system also changes all the time, especially those in a lower orbit. It is not easy to introduce defocus diversity the magnitude of which is enough to guarantee the uniqueness of the solution. During this process, it is possible that the perturbation state of the system can change by some extent. The vibration conditions at different times are also different. This can definitely introduce some error in phase retrieval wavefront sensing.

B. Multifield Phase Retrieval Wavefront Sensing Concept

To achieve the goal of recovering the wavefront phase of the system without any additional instruments or operations (except for the detector), in this part we will propose a new phase retrieval concept for wavefront sensing in space telescopes.

Space telescopes are completely free from atmospheric turbulence effects. They are only subject to the misalignments and figure errors of the system. In this case, on one hand, the aberrations at different field points are typically different, especially astigmatism. The astigmatic aberration fields for two different types of telescope with misalignments are illustrated in Fig. 2. We can easily recognize that the astigmatism varies with field in both of the two cases. In other words, if several intensity measurements are obtained at different field positions, there can be phase diversity between these intensity measurements. On the other hand, while the aberrations at different field positions are different, they are not completely random. In effect, the aberrations induced by misalignments or figure errors at different field positions have deep inherent relationships. In the presence of misalignments and figure errors, each aberration type can exhibit a characteristic aberration field dependency [24–33]. Here we take the astigmatism as an example again. As shown in Fig. 2, the misalignment astigmatic aberration field in two-mirror telescopes exhibits a bi-nodal characteristic [27]; in three-mirror anastigmatic (TMA) telescopes, it is field-linear and field-asymmetric [28].

Therefore, here we present a new phase retrieval concept for wavefront sensing in space telescopes. In this concept, the intensity measurements needed for phase retrieval methods are obtained from different field positions. Since the phase aberrations at different field positions are different, these intensity measurements have phase diversities between them, which are indispensable in guaranteeing the uniqueness of the solution. On the other hand, while the phase diversities between different field positions are unknown to us, the phase aberrations at different field positions have inherent relationships, which present the possibility of realizing this phase retrieval concept.

Since the intensity measurements are obtained at multiple field positions, we call this concept as the multifield phase retrieval concept. The comparison between this new concept and the traditional multiplane phase retrieval concept is shown in Fig. 3. The main difference that lies between them is the way to obtain intensity measurements with phase diversity. Since intensity measurements at different field positions can be obtained simultaneously from one exposure, this new concept can eliminate the need for additional instruments or operations. We should point out that there has been one existing method that uses multifield intensity measurements to determine the wavefront aberrations of the system [34–37]. In this method, all spot size and ellipticity patterns across the field are expanded in terms of standard Zernike polynomials. Such information can reduce and constrain the set of functions fitted to the measured spot sizes and ellipticities. Optical aberrations in the field

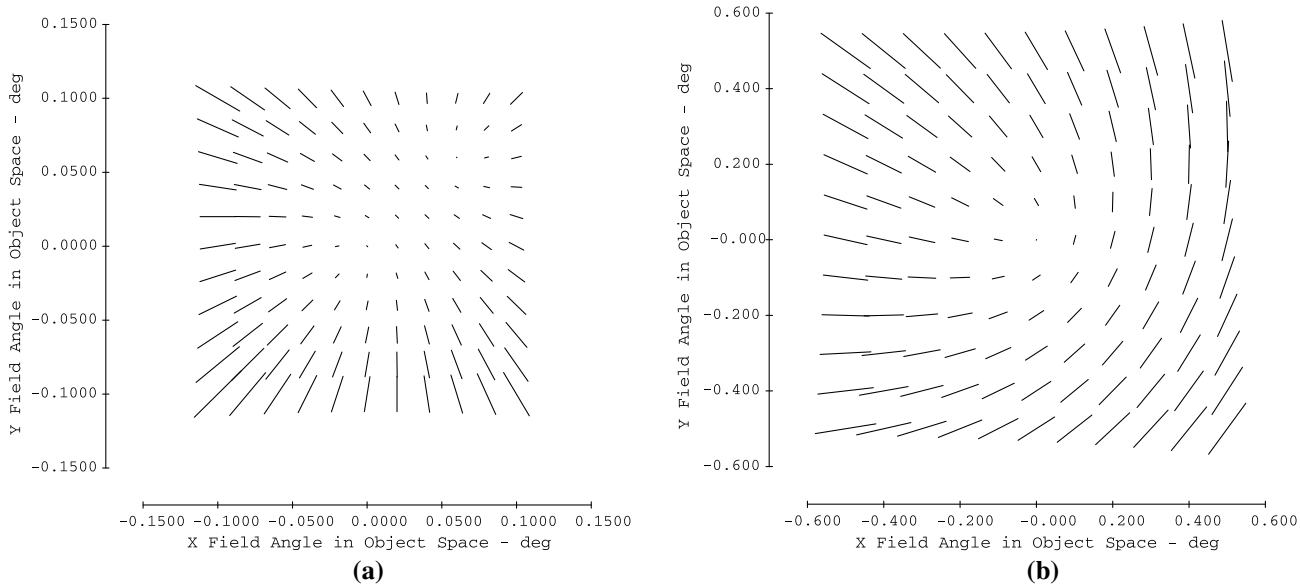

Fig. 2. Full-field displays (FFDs) for the astigmatism (Z5/Z6) in (a) a two-mirror telescope and (b) a TMA telescope when they are in a misaligned state. Each line in the FFDs represents the magnitude and orientation of astigmatism for a certain field point. On one hand, we can clearly recognize that the astigmatism varies with field in both of the two cases. On the other hand, this aberration also exhibits a characteristic field dependency in each case.

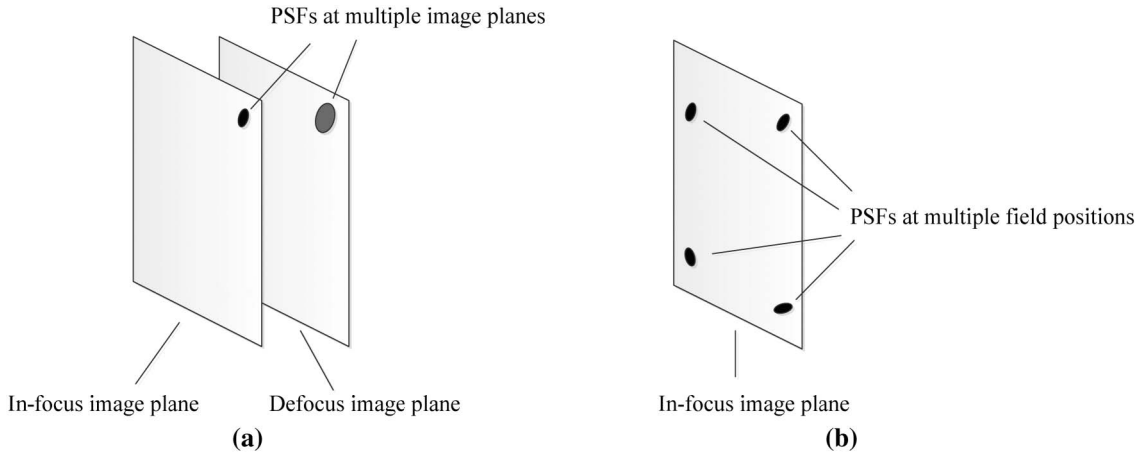

Fig. 3. Comparison of (a) the traditional multiplane phase retrieval concept and (b) the new multifield phase retrieval concept proposed in this paper. The black spots in the figure represent the intensity measurements (PSFs) with the phase diversity needed for phase retrieval algorithms. In the multifield phase retrieval concept, the intensity measurements with phase diversity can be directly obtained simultaneously with one exposure, without the need for any additional operation or instrument.

can then be determined by fitting an analytical model to the ellipticity and spot size pattern. However, this method is very different from the phase retrieval wavefront sensing methods and its accuracy is relatively low. We cannot directly extend this method to the multifield phase retrieval concept. On the other hand, the fact that there exists one method of using multifield intensity measurements to determine the aberrations of the system also signifies that it is possible to perform phase retrieval methods with multifield intensity measurements.

Note that when there is a little perturbation in the system, the phase diversities between different field positions are very small, especially for TMA telescopes, which may be not enough for guaranteeing the uniqueness of the solution. In this case, we can easily further introduce defocus diversity by translating the detector (wavefront sensor) and fix it in advance. During the wavefront sensing process, the positions of these detectors are unchanged. Therefore, still no additional instruments or operations are needed in this process. Three specific forms for the setting of the wavefront sensors relevant to the proposed multifield phase retrieval wavefront sensing concept are shown in Fig. 4. For two-mirror telescopes, the astigmatisms are not well corrected even at the nominal state, which can provide the

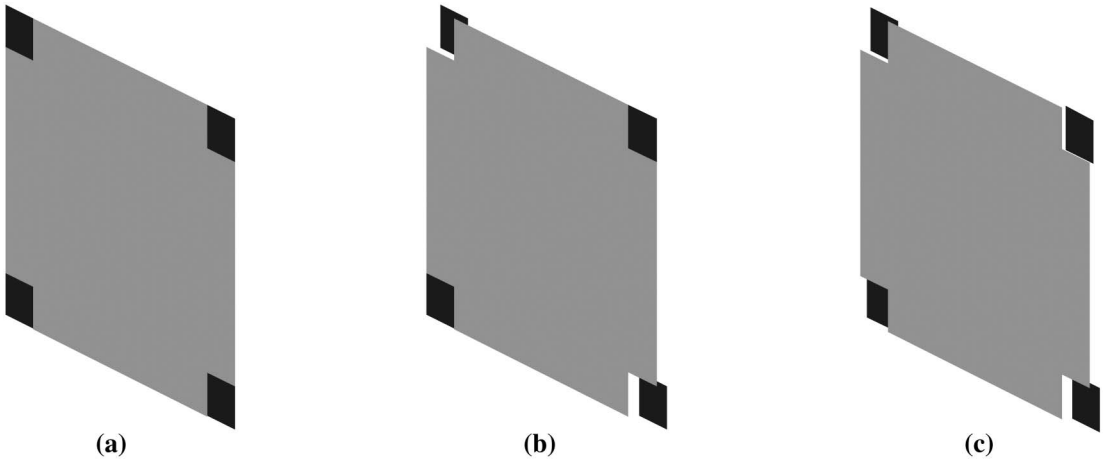

Fig. 4. Three specific forms for the setting of the wavefront sensors relevant to the proposed multifield phase retrieval wavefront sensing concept. The gray region in each form represents the science field of view, and the black regions at the corner represent the wavefront sensor. In (a), all the wavefront sensors are located at the in-focus image plane. In (b), two wavefront sensors are located at the in-focus image plane and the other two at the same defocus image plane. In (c), the four wavefront sensors are located at four different focal image planes.

phase diversities between intensity measurements at different field positions. For this case, we can directly use the first form of multifield phase retrieval concept in Fig. 4. For TMA telescopes, we can use the other two forms of the multifield phase retrieval concept, where known defocus diversity is also added between intensity measurements at different field positions.

3. FIELD DIVERSITY PHASE RETRIEVAL WAVEFRONT SENSING METHOD FOR MONOLITHIC MIRROR SPACE TELESCOPES

In the previous section, we propose a multifield phase retrieval concept. In this section, we will propose the corresponding algorithm to realize this wavefront sensing concept. We first briefly review the current phase diversity phase retrieval algorithm, which was first proposed by Gonsalves in 1979 and extended by others [7–9]. Then we present a modified algorithm relevant to the multifield phase retrieval concept to account for the unknown phase diversities between the intensity measurements at multiple field positions, based on an in-depth interpretation of the aberration field characteristics of large telescopes with perturbations. To help understand the proposed algorithm, we first present some deep discussions on the current algorithm. Then we make comparisons between the two algorithms and analyze the similarities and differences between them. Specifically, for both of the two algorithms, there is one set of unknown parameters corresponding to several known intensity measurements with phase diversity. In the current algorithm, this set of unknown parameters are aberration coefficients for a certain field point. However, in the modified algorithm proposed in this paper, the set of unknown parameters represent the coefficients for the field dependencies of different aberration types over the whole field.

A. Current Phase Diversity Phase Retrieval Algorithm

Let us suppose that the object is illuminated with noncoherent quasi-monochromatic light, and the imaging system is a linear shift-invariant system. The intensity distribution of the image plane with Gaussian noise can be modeled as

$$d_k(\boldsymbol{r}) = o(\boldsymbol{r}) * s_k(\boldsymbol{r}) + n_k(\boldsymbol{r}), \tag{1}$$

where $*$ denotes the convolution operation, $\boldsymbol{r}$ is a two-dimensional position vector in the image plane, $o(\boldsymbol{r})$ is the object, $d_k(\boldsymbol{r})$ is the kth detected diversity image, $s_k(\boldsymbol{r})$ is the kth point-spread function (PSF), and $n_k(\boldsymbol{r})$ is the Gaussian noise in the kth image. With the condition of near field, the point-spread function associated with the kth diversity image is given by

$$s_k(\boldsymbol{r}) = |F^{-1}\{P(\rho)\exp[\varphi_k(\rho)]\}|^2, \tag{2}$$

where F^{-1} denotes the inverse Fourier transform, ρ is a two-dimensional position vector in the pupil plane, $P(\rho)$ is the binary aperture function with a value of 1 inside the pupil and 0 outside, and $\varphi_k(\rho)$ represents the wavefront phase associated with the kth intensity measurement. In the current phase diversity algorithm, $\varphi_k(\rho)$ can further be expressed as

$$\varphi_k(\rho) = \phi(\rho) + \Delta_k(\rho), \tag{3}$$

where $\phi(\rho)$ is the unknown wavefront aberration to be estimated, and $\Delta_k(\rho)$ is the deliberately introduced kth phase diversity, which is usually known to us.

To evaluate the difference between the diversity images predicted by the imaging model of the optical system and those directly collected, an error metric can be defined as

$$E = \sum_{k=1}^{K}\sum_{\boldsymbol{r}}[d_k(\boldsymbol{r}) - o(\boldsymbol{r}) * s_k(\boldsymbol{r})]^2. \tag{4}$$

According to the convolution theorem and the Parseval theorem, this error metric can be rewritten in the frequency domain as

$$E = \sum_{k=1}^{K}\sum_{\boldsymbol{u}}[D_k(\boldsymbol{u}) - O(\boldsymbol{u}) * S_k(\boldsymbol{u})]^2, \tag{5}$$

where $\boldsymbol{u}$ is a two-dimensional spatial frequency coordinate, $D_k(\boldsymbol{u})$, $O(\boldsymbol{u})$ and $S_k(\boldsymbol{u})$ denote the Fourier transforms of $d_k(\boldsymbol{r})$, $o(\boldsymbol{r})$ and $s_k(\boldsymbol{r})$, respectively.

In order to reduce the dimensions of the parameter space over which a numerical optimization is performed, the partial differential of the error metric E with respect to the object frequency spectrum O is set to zero. In this case, we can obtain

$$O(\boldsymbol{u}) = \frac{\sum_{k=1}^{K} D_k(\boldsymbol{u}) S_k^*(\boldsymbol{u})}{\sum_{k=1}^{K} |S_k(\boldsymbol{u})|^2}, \qquad \sum_{k=1}^{K} |S_k(\boldsymbol{u})|^2 \neq 0. \tag{6}$$

$S_k^*(\boldsymbol{u})$ in Eq. (6) represent the complex conjugate of $S_k(\boldsymbol{u})$.

Substitution of $O(\boldsymbol{u})$ into E yields

$$E = \sum_{k=1}^{K} \sum_{\boldsymbol{u}} |D_k(\boldsymbol{u})|^2 - \sum_{\boldsymbol{u}\in\chi} \frac{\left| \sum_{k=1}^{K} D_k(\boldsymbol{u}) S_k^*(\boldsymbol{u}) \right|^2}{\sum_{k=1}^{K} |S_k(\boldsymbol{u})|^2}, \tag{7}$$

where χ represents a set of spatial frequencies $\boldsymbol{u}$,

$$\chi = \left\{ \boldsymbol{u} \middle| \sum_{k=1}^{K} |S_k(\mathbf{u})|^2 \neq 0 \right\}. \tag{8}$$

The unknown wavefront aberration is usually expanded on a finite set of Fringe Zernike polynomials,

$$\phi(\boldsymbol{\rho}) = \sum_{j=4}^{N} C_j Z_j(\boldsymbol{\rho}). \tag{9}$$

The coefficients C_1–C_3 stand for piston and tilt of the wavefront aberration, which have no effect on the quality of the image. The error metric E is therefore defined by a multidimensional parameter space:

$$\boldsymbol{a} = [C_4, C_5, \ldots, C_N]. \tag{10}$$

For a group of given parameters $\boldsymbol{a}$, the error metric $E(\boldsymbol{a})$ can be calculated. The problem of reconstructing aberration coefficients of the wavefront phase can be transferred to searching the coefficient set for which the error metric presented by Eq. (7) is a global minimum. A series of nonlinear optimization algorithms can help us to achieve this goal [38–40].

B. Field Diversity Phase Retrieval Algorithm

Before we propose the modified phase diversity algorithm for the multifield phase retrieval concept, we here first present a deep discussion on the current phase diversity algorithm presented above. We can recognize that one key point of the phase diversity algorithm is that there is only one set of unknown parameters that is needed to determine, while there are usually more than one intensity measurement with phase diversity that are utilized to establish the error metric. As mentioned in Section 1, the mathematical mapping from the set of all possible pupil phase screens to the set of all possible intensity distributions is a many-to-one mapping. Therefore, to invert this mapping and guarantee the uniqueness of the solution for the wavefront phase, we need increase the number of intensity measurements while guaranteeing that no additional sets of unknown parameters are introduced. To this end, we usually deliberately introduce phase diversity to the system to obtain more intensity measurements. Besides, this phase diversity is usually known to us, and therefore no additional sets of unknown parameters are introduced.

However, for the multifield phase retrieval concept, the phase diversities between different intensity measurements at different field positions are typically unknown to us when the system is perturbed (i.e., the elements of the system are misaligned or deformed). In this case, we cannot directly apply the current phase diversity phase retrieval algorithm to recover the wavefront phase of the system. The reason is that while the number of the intensity measurements is more than one, the number of the set of unknown parameters is more than one, too. In other words, the uniqueness of the solution cannot be guaranteed.

Therefore, we can recognize that the key to realizing the multifield phase retrieval wavefront sensing concept is how to use one set of unknown parameters to express the phase aberrations at multiple field points (the number of the parameters in this set should also be comparable to the current phase diversity algorithm). To this end, we here first express the coefficient of each aberration type for a certain field position (x_k, y_k) as a combination of two components, i.e., that in the nominal state and that induced by perturbations (misalignments and figure errors),

$$C_j(x_k, y_k) = C_j^{(N)}(x_k, y_k) + C_j^{(P)}(x_k, y_k), \tag{11}$$

where (x_k, y_k) represents the position coordinate of the kth intensity measurement in the field, $C_j^{(N)}(x_k, y_k)$ represents the jth Zernike aberration coefficient when the system is in the nominal state, and $C_j^{(P)}(x_k, y_k)$ represents the net contribution to the jth Zernike aberration coefficient induced by perturbations. Then we continue to express these two components as a function of the field position,

$$\begin{aligned} C_j^{(N)}(x_k, y_k) &= n_j^{(0,0)} + n_j^{(1,0)} x_k + n_j^{(0,1)} y_k + n_j^{(1,1)} x_k y_k + \ldots, \\ C_j^{(P)}(x_k, y_k) &= p_j^{(0,0)} + p_j^{(1,0)} x_k + p_j^{(0,1)} y_k + p_j^{(1,1)} x_k y_k + \ldots, \end{aligned} \tag{12}$$

or

$$\begin{aligned} C_j^{(N)}(x_k, y_k) &= \sum_{s=0} \sum_{t=0} n_j^{(s,t)} x_k^s y_k^t, \\ C_j^{(P)}(x_k, y_k) &= \sum_{s=0} \sum_{t=0} p_j^{(s,t)} x_k^s y_k^t, \end{aligned} \tag{13}$$

where $n_j^{(s,t)}$ and $p_j^{(s,t)}$ are the corresponding coefficients for a certain type of field-dependency factor, $x_k^s y_k^t$. In this case, the $\varphi_k(\boldsymbol{\rho})$ in Eq. (2) should be rewritten as

$$\varphi_k(\boldsymbol{\rho}) = \sum_{j=4}^{N} \sum_{s=0} \sum_{t=0} (n_j^{(s,t)} + p_j^{(s,t)}) x_k^s y_k^t Z_j(\rho). \tag{14}$$

Note that the field dependency of the Fringe Zernike aberration coefficients in the nominal state are usually known to us. For example, for two-mirror telescopes, we can only consider the third-order aberrations. In this case, we can write

$$
\begin{aligned}
C_4^{(N)}(x_k,y_k) &= \frac{1}{2}W_{220M}(x_k^2+y_k^2),\\
C_5^{(N)}(x_k,y_k) &= \frac{1}{2}W_{222}(x_k^2-y_k^2),\\
C_6^{(N)}(x_k,y_k) &= W_{222}x_k y_k,\\
C_7^{(N)}(x_k,y_k) &= \frac{1}{3}W_{131}x_k,\\
C_8^{(N)}(x_k,y_k) &= \frac{1}{3}W_{131}y_k,\\
C_9^{(N)}(x_k,y_k) &= \frac{1}{6}W_{040},\\
C_j^{(N)}(x_k,y_k) &\approx 0, \qquad j>9,
\end{aligned}
\tag{15}
$$

where W_{220M}, W_{222}, W_{131}, and W_{040} represent the aberration coefficients for medial focal surface, astigmatism, coma, and spherical aberration, respectively. The correspondence between Seidel coefficients and Fringe Zernike coefficients has been considered in Eq. (15) [41]. For TMA telescopes, the field dependencies of different aberration types are a little complicated to express. However, the aberration coefficients of a nominal system for a certain field point are usually known to us. We can directly obtain them from the optical simulation software and make a reference table.

Therefore, now there is only one set of unknown parameters that is needed to express the wavefront aberrations at multiple field points, i.e.,

$$
\begin{aligned}
&p_4^{(0,0)}, p_4^{(1,0)}, p_4^{(0,1)}, p_4^{(1,1)}, \ldots,\\
&p_5^{(0,0)}, p_5^{(1,0)}, p_5^{(0,1)}, p_5^{(1,1)}, \ldots,\\
&\ldots,\\
&p_N^{(0,0)}, p_N^{(1,0)}, p_N^{(0,1)}, p_N^{(1,1)}, \ldots.
\end{aligned}
\tag{16}
$$

We can see that while in this case there is only one set of parameters, there are too many unknown parameters in this set that are needed to be determined. Therefore, we should continue to reduce the number of the parameters that is needed to express the aberration fields of the optical systems when they are perturbed.

In effect, based on a deep understanding of the net aberration fields induced by misalignments and figure errors [24–33], the expression for $C_j^{(P)}(x_k,y_k)$ can be greatly simplified. Space telescopes are completely free of atmospheric turbulence effects and the aberrations of the system are mainly induced by misalignments and figure errors of the system. As known to us, for on-axis telescopes, lateral misalignments mainly affect lower-order nonrotationally symmetric aberrations, such as astigmatism and coma; axial misalignments mainly introduced lower-order rotationally symmetric aberrations, such as defocus and a little spherical aberration; the primary mirror figure errors are mainly astigmatism and trefoil, which induce the corresponding aberrations to the system. The higher-order ($j>11$) aberrations are usually very small and we can neglect them (proper reduction of the number of the unknown parameters can also decrease the possibility of being trapped in a local minimum). On the other hand, most of these net aberration contributions induced by misalignments and figure errors have a very low order of field dependency, and some of them do not have any field dependency, i.e., they are field constant. Therefore, based on the understanding of the net aberration fields induced by misalignments and figure errors, $C_j^{(P)}(x_k,y_k)$ can be rewritten as

$$
\begin{aligned}
C_4^{(P)}(x_k,y_k) &= J_1x_k + J_2y_k + J_3,\\
C_5^{(P)}(x_k,y_k) &= J_4x_k + J_5y_k + J_6,\\
C_6^{(P)}(x_k,y_k) &= -J_5x_k + J_4y_k + J_7,\\
C_7^{(P)}(x_k,y_k) &= J_8,\\
C_8^{(P)}(x_k,y_k) &= J_9,\\
C_9^{(P)}(x_k,y_k) &= J_{10},\\
C_{10}^{(P)}(x_k,y_k) &= J_{11},\\
C_{11}^{(P)}(x_k,y_k) &= J_{12},\\
C_j^{(P)}(x_k,y_k) &\approx 0, \qquad j>11.
\end{aligned}
\tag{17}
$$

Here we no longer use the set of parameters, $p_j^{(s,t)}$, to express the field dependency of the net aberration contributions induced by perturbations. The parameters in this set are not completely independent. As we can recognize from Eq. (17), $p_5^{(1,0)} = p_6^{(0,1)}$ and $p_5^{(0,1)} = -p_6^{(1,0)}$. Note that here we do not consider the figure errors of the secondary mirrors. If there are considerable figure errors (especially trefoil errors) on the secondary mirrors, Eq. (17) should be modified. Trefoil errors at secondary mirrors can introduce a field-linear, field-conjugate astigmatism to the system [30–32], which will be coupled with the field-linear astigmatism induced by lateral misalignments. In this case, we need to use different parameters to represent $p_5^{(1,0)}$ and $p_6^{(0,1)}$, as well as $p_5^{(0,1)}$ and $p_6^{(1,0)}$, i.e., these parameters become independent. However, generally we can neglect this effect.

Therefore, we can use a new set of parameters, J_1-J_{12}, to express the field dependency of the net aberration contributions induced by perturbations. In this case, the error metric presented in Eq. (7) is now defined by a new multidimensional parameter space:

$$
\boldsymbol{b} = [J_1, J_2, \ldots, J_{12}]. \tag{18}
$$

For a group of given parameters $\boldsymbol{b}$, we can express the phases $\varphi_k(\rho)$ associated with the intensity measurements at multiple field positions (the field positions of these intensity measurements are usually known to us). The corresponding error metric $E(\boldsymbol{b})$ can also be calculated. By searching the global minimum of this error metric, we can obtain a set of $\boldsymbol{b}$. Then we can determine the aberration coefficients at an arbitrary position in the field with Eqs. (11) and (17).

To facilitate a deep understanding of this modified phase diversity algorithm relevant to the multifield phase retrieval concept, we here make a comparison between the two phase diversity algorithms presented in this section. We first present the similarities between them, which are listed below:

(1) Both of these two algorithms belong to the parametric or model-based optimization phase retrieval methods.

(2) The error metric used by these two algorithms is also the same.

(3) In both of the two algorithms, one set of unknown parameters is enough to express the phases associated with multiple intensity measurements with phase diversity between them.

Then we concentrate on the differences between them, which are listed below:

(1) These two algorithms are associated with two different phase retrieval concepts.

(2) In the current phase diversity algorithm, a known phase diversity between different intensity measurements is usually needed, while in the modified algorithm, the phase diversities between different intensity measurements are usually known.

(3) In the current phase diversity algorithm, the unknown parameters are the aberration coefficients for one certain field point, while in modified algorithm, the unknown parameters are the coefficients for the field dependencies of different aberration types over the whole field.

(4) Using the current phase diversity algorithm, we can obtain the aberration coefficients for one certain field point at one time, while using the modified algorithm, we can determine aberration coefficients over the whole field at one time, i.e., the aberrations at different field points can be determined simultaneously. Therefore, the modified algorithm has a very high efficiency for wavefront sensing in space telescopes. In practice, wavefront aberrations at several certain field points are usually needed. However, it is very likely that no suitable star is located at these field positions. In this case, we usually need to adjust the boresight to locate a star bright enough at these deterministic field positions. Note that the efficiency of the current defocus diversity phase retrieval method is already low due to the additional operations to obtain defocus diversity. The adjustment of the boresight can further lower the efficiency for wavefront sensing in space telescopes. However, in the modified algorithm presented in this paper, several intensity measurements at several arbitrary field positions are enough to determine the aberrations over the whole field. In other words, the aberrations at the several deterministic field positions can be determined at the same time without any additional operations, including the adjustment of the boresight. Therefore, the new multifield phase retrieval wavefront sensing concept and the modified phase diversity algorithm associated with it can greatly improve the efficiency of wavefront sensing in space telescopes.

To distinguish the current phase diversity algorithm and the modified one presented in this paper, we call this modified algorithm as the field diversity phase retrieval algorithm since the intensity measurements are obtained from different field positions and the phase diversities between different intensity measurements are mainly induced by the diversities in field position.

In this section, we mainly take the specific form of the multifield phase retrieval concept presented in Fig. 4(a) as an example to propose the relevant field diversity phase retrieval algorithm. This algorithm can easily be extended to other forms of the multifield phase retrieval concept presented in Fig. 4, where each wavefront sensor at the corner can be axially displaced with a different distance to further introduce phase diversity between those intensity measurements at multiple fields. In this case, Eq. (14) should be rewritten as

$$\varphi_k(\boldsymbol{\rho}) = \sum_{j=4}^{N}\sum_{s=0}\sum_{t=0}(n_j^{(s,t)} + p_j^{(s,t)})x_k^s y_k^t Z_j(\boldsymbol{\rho}) + \Delta_k(\boldsymbol{\rho}), \tag{19}$$

where $\Delta_k(\boldsymbol{\rho})$ is the kth diversity phase further introduced by axially displacing the detector for the intensity measurement at the kth field position. We stress again that while we here further introduce defocus diversity, this phase diversity is introduced in advance, not during the observing period. The wavefront sensor at multiple field positions will be fixed after they are translated, and therefore, still no additional instruments or operations are needed in the wavefront sensing process.

4. SIMULATIONS

In this section, detailed simulations will be performed to verify the feasibility and accuracy of the proposed field diversity phase retrieval method under different perturbation conditions and noise levels. Specifically, the field diversity phase retrieval method will be utilized to recover the wavefront aberrations of a two-mirror telescope (Hubble Space Telescope) and a TMA telescope [which is a preliminary optical configuration for the Supernova/Acceleration Probe (SNAP) mission]. The simulation process for each case is listed below:

(1) Introduction of perturbation. A perturbation state is generated randomly within certain perturbation ranges and then introduced into the optical system in the optical simulation software.

(2) Acquisition of PSFs at multiple field positions. Four field positions are selected randomly within certain areas near the four corners of the field of view. For each selected field position, the aberration coefficients are obtained from optical simulation software. Then the PSF at this field position can be calculated. This PSF can also be directly obtained from the optical simulation software.

(3) Addition of noise. A certain intensity of additive zero-mean Gaussian white noise will be added to each PSF, where the noise is specified by the ratio of the standard deviation of the noise to the peak value in the noiseless PSF image. These calculated PSFs with noise are used to simulate the true intensity measurements obtained from multiple field positions.

(4) Reconstruction of the wavefront. Since several intensity measurements (PSFs) from multiple field positions are available now, the proposed field diversity phase retrieval method can be used to recover the wavefront of the system. Note that certain nonlinear optimization methods must be needed in this process. We prefer to use the method presented in [40], which can effectively reduce the possibility of being trapped in a local minimum.

(5) Evaluation of the accuracy. Four deterministic field positions are selected. These positions are usually different from those field positions that provide the PSFs. The root mean square deviation (RMSD) between the real aberration coefficients and those recovered by the proposed method for the four field points is used to evaluate the accuracy of the method, which is expressed as

$$\mathrm{RMSD} = \sqrt{\frac{\sum_{m=1}^{4}\sum_{j=4}^{11}[C_j^{(0)}(x_m,y_m) - C_j^{(1)}(x_m,y_m)]^2}{4\times 8}}, \tag{20}$$

where $C_j^{(0)}(x_m, y_m)$ represents the jth Fringe Zernike coefficient that is read from optical simulation software at the field position (x_m, y_m), and $C_j^{(1)}(x_m, y_m)$ is the corresponding coefficient recovered by the proposed method.

Here the field points used to provide intensity measurements (PSFs) and the field points used to evaluate the accuracy of the proposed method are different. This is because in practice it is very likely that no suitable star is located at the specified field points and we want to show that other positions of the intensity measurements can be used to recover the wavefront at the specified field positions.

(6) Comparison of the accuracy with the current defocus diversity phase retrieval method under different perturbation conditions and noise levels. Specifically, for three different perturbation ranges and noise levels, we will compare the accuracy of the field diversity and defocus diversity phase retrieval method with the Hubble Space Telescope and the preliminary SNAP telescope.

A. Case of the Hubble Space Telescope

We first use the Hubble space telescope (HST) to demonstrate the accuracy of the field diversity phase retrieval method. The optical prescription and layout of the system are presented in Appendix A. The perturbations of the system considered in this paper include the axial and lateral misalignments of the secondary mirror and detector (with reference to the primary mirror) and the figure errors in the primary mirror. Three different perturbation ranges and three noise levels are considered here, as shown in Table 1. In Case 1–Case 3, the perturbation range increases in sequence, but no noise is considered; in Case 3–Case 5, the perturbation ranges are the same, but the noise level increases in sequence. Therefore, by analyzing the results for Case 1–Case 3, we can know the effect of perturbation range on the accuracy of the different phase retrieval methods. Similarly, by analyzing the results for Case 3–Case 5, we can know the sensitivities of different phase retrieval methods to the noise level.

In Table 1, *XDE* and *YDE* are the surface vertex decenters in the $x-z$ and $y-z$ plane, respectively, and *BDE* and *ADE* are the surface tip-tilts in the $x-z$ and $y-z$ plane, respectively. For simplicity, here we assume that the misalignment ranges of the secondary mirror and the detector are the same in each case. We use the Fringe Zernike polynomials to express the figure errors of the primary mirror. These errors include astigmatism, coma, spherical and trefoil figure errors, which correspond to $C_5^{(F)}$–$C_{11}^{(F)}$ (here $C_i^{(F)}$ is the ith Fringe Zernike coefficient used to express the figure error of the primary mirror). We here also assume that they have the same perturbation range in each case.

In the simulations, the four field positions used to provide intensity measurements for the field diversity method are selected randomly from four areas at the four corners of the field of view. They are $(-0.1° \pm 0.01°, -0.1° \pm 0.01°)$, $(-0.1° \pm 0.01°, 0.1° \pm 0.01°)$, $(0.1° \pm 0.01°, -0.1° \pm 0.01°)$, and $(0.1° \pm 0.01°, 0.1° \pm 0.01°)$. The four field points used to evaluate the accuracy of the two phase retrieval methods are $(-0.1°, -0.1°)$, $(-0.1°, 0.1°)$, $(0.1°, -0.1°)$, and $(0.1°, 0.1°)$.

For each of the five cases presented in Table 1, 100 perturbations states will be introduced into the system within the specified perturbation ranges. For each perturbation state, the simulation process presented above will be performed, and the RMSD will be calculated to evaluate the accuracy. Note that in the simulation process, the aberration coefficients of the nominal system at different field positions are obtained from optical simulation software, because we find that the accuracy of Eq. (15) is not high enough even for a two-mirror telescope (fifth-order aberration coefficients are not considered in this equation).

The accuracy of the field diversity method within different perturbation ranges (Case 1–Case 3) and under different noise levels (Case 3–Case 5) is shown in Figs. 5(a) and 5(b), respectively. The accuracy of the defocus diversity method within different perturbation ranges (Case 1–Case 3) and under different noise levels (Case 3–Case 5) is shown in Figs. 6(a) and 6(b), respectively. By comparing Figs. 5 and 6, we can obtain the following results:

(1) The accuracy of the field diversity method is lower than the defocus diversity method in the absence of noise. The main reason is that in the mathematical presentation of the field diversity method, we neglect those aberration contributions with a high-order field dependency that are induced by perturbations. The focus diversity method does not include this approximation, and its accuracy is higher.

(2) We can also see from Fig. 5(a) that the accuracy of the field diversity method decreases as the perturbation range increases. The main reason is that as the perturbation range increases, those aberration contributions with a high-order field dependency that are neglected in the field diversity method also increase. Similarly, the focus diversity method does not include this approximation, so its accuracy is not affected by change in the perturbation range.

(3) On the other hand, importantly, we can recognize that the accuracy of our field diversity method is less sensitive to noise compared to the defocus diversity method. The main reason is that the knowledge of the field dependencies of different aberration types induced by perturbations is inherent in the field diversity method. This knowledge can put a

Table 1. Perturbation Ranges of the HST and Noise Levels Considered in the Simulations

	XDE, *YDE*(mm)	*ADE*, *BDE*(deg)	*ZDE*(mm)	$C_5^{(F)}$ – $C_{11}^{(F)}$ (λ)[a]	Noise Level
Case 1	[−0.02,0.02]	[−0.002,0.002]	[−0.01,0.01]	[−0.01,0.01]	0
Case 2	[−0.05,0.05]	[−0.005,0.005]	[−0.02,0.02]	[−0.02,0.02]	0
Case 3	[−0.1,0.1]	[−0.01,0.01]	[−0.04,0.04]	[−0.05,0.05]	0
Case 4	[−0.1,0.1]	[−0.01,0.01]	[−0.04,0.04]	[−0.05,0.05]	0.5%
Case 5	[−0.1,0.1]	[−0.01,0.01]	[−0.04,0.04]	[−0.05,0.05]	1%

[a]$\lambda = 632.8$ nm.

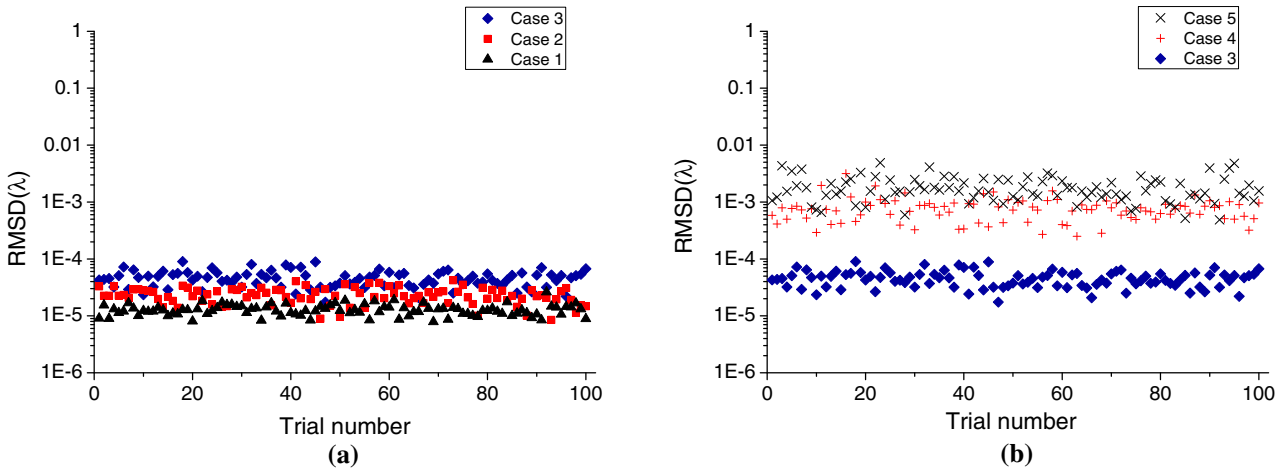

Fig. 5. RMSD between the real aberration coefficients at the four specified field points and those recovered by the field diversity phase retrieval method under (a) different perturbation conditions and (b) different noise levels for the HST. Here RMSD is measured in λ ($\lambda = 632.8$ nm).

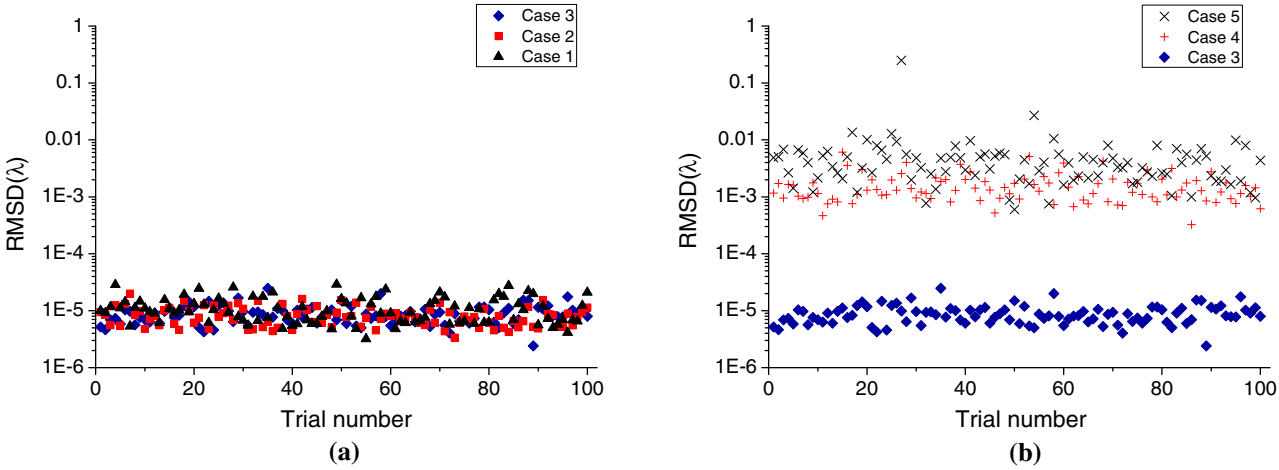

Fig. 6. RMSD between the real aberration coefficients at the specified field points and those recovered by the defocus diversity phase retrieval method under (a) different perturbation conditions and (b) different noise levels for the HST. Here RMSD is measured in λ ($\lambda = 632.8$ nm).

constraint on the recovered aberration coefficients and reduce the impact of noise, especially when intensity measurements at more than two field points are used to perform the field diversity method. There is no such constraint in the defocus diversity method, and it is more sensitive to noise.

B. Case of the Preliminary SNAP Telescope

We continue to the preliminary SNAP telescope to use demonstrate the accuracy of the field diversity phase retrieval method. The optical prescription and layout of the system are presented in Appendix A. The perturbations of the system considered in this paper include the axial and lateral misalignments of the secondary mirror, tertiary mirror, and detector (with reference to the primary mirror), and the figure errors in the primary mirror. Similarly, three different perturbation ranges and three noise levels are considered here, as shown in Table 2.

Table 2. Perturbation Ranges of the Preliminary SNAP Telescope and Noise Levels Considered in the Simulations

	XDE, *YDE*(mm)	*ADE*, *BDE*(deg)	*ZDE*(mm)	$C_5^{(F)} - C_{11}^{(F)}(\lambda)^a$	Noise Level
Case 1	[−0.02,0.02]	[−0.002,0.002]	[−0.005,0.005]	[−0.01,0.01]	0
Case 2	[−0.05,0.05]	[−0.005,0.005]	[−0.01,0.01]	[−0.02,0.02]	0
Case 3	[−0.1,0.1]	[−0.01,0.01]	[−0.02,0.02]	[−0.05,0.05]	0
Case 4	[−0.1,0.1]	[−0.01,0.01]	[−0.02,0.02]	[−0.05,0.05]	0.5%
Case 5	[−0.1,0.1]	[−0.01,0.01]	[−0.02,0.02]	[−0.05,0.05]	1%

[a] $\lambda = 632.8$ nm.

Table 3. Optical Prescription for the Hubble Space Telescope

Surface	Radius(mm)	Conic	Thickness(mm)
M1(stop)	−11040.00	−1.00230	−4906.07
M2	−1358.00	−1.49686	6406.20
FP	−631.08		

Table 4. Optical Prescription for the Preliminary SNAP Telescope

Surface	Radius(mm)	Conic	Thickness(mm)	Tilt about X
M1(stop)	−5476.9498	−0.9745	−2240.6678	0
M2	−1249.3071	−2.02415	3800	0
M3	−1610.9095	−0.54897	−991.4634	0
M4	FLAT	\	−1008.5366	45°
FP	FLAT	\	\	\

For simplicity, in the simulations we still consider the misalignment ranges of the secondary mirror, tertiary mirror, and detector are the same in each case.

In the simulations, the four field positions used to provide intensity measurements for the field diversity method are selected randomly from four areas at the four corners of the field of view. They are $(-0.5° \pm 0.05°, -0.5° \pm 0.05°)$, $(-0.5° \pm 0.05°, 0.5° \pm 0.05°)$, $(0.5° \pm 0.05°, -0.5° \pm 0.05°)$, and $(0.5° \pm 0.05°, 0.5° \pm 0.05°)$. The four field points used to evaluate the accuracy the two phase retrieval methods are $(-0.5°, -0.5°)$, $(-0.5°, 0.5°)$, $(0.5°, -0.5°)$, and $(0.5°, 0.5°)$.

For each of the five perturbation cases presented in Table 2, 100 perturbations states will be introduced into the system within the specified perturbation ranges. For each perturbation state, the simulation process will be performed, and the RMSD will be calculated to evaluate the accuracy.

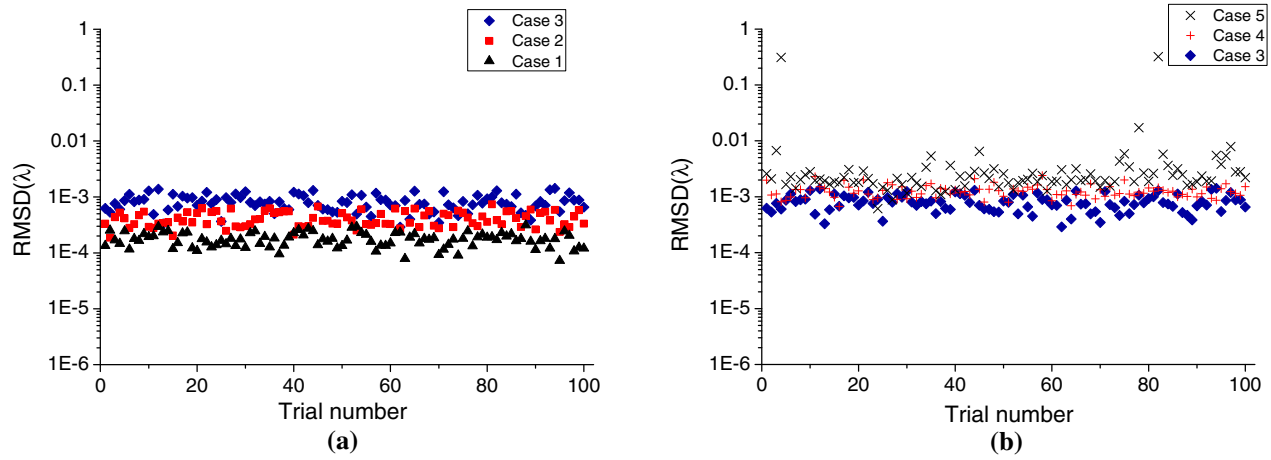

Fig. 7. RMSD between the real aberration coefficients at the specified field points and those recovered by the field diversity phase retrieval method under (a) different perturbation conditions and (b) different noise levels for the preliminary SNAP telescope. Here RMSD is measured in λ ($\lambda = 632.8$ nm).

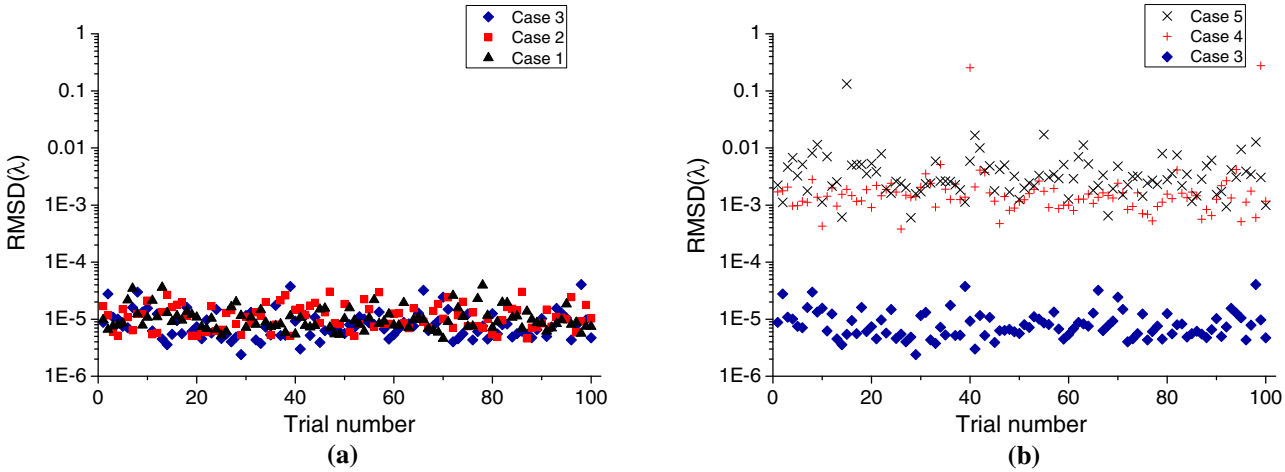

Fig. 8. RMSD between the real aberration coefficients at the specified field points and those recovered by the defocus diversity phase retrieval method under (a) different perturbation conditions and (b) different noise levels for the preliminary SNAP telescope. Here RMSD is measured in λ ($\lambda = 632.8$ nm).

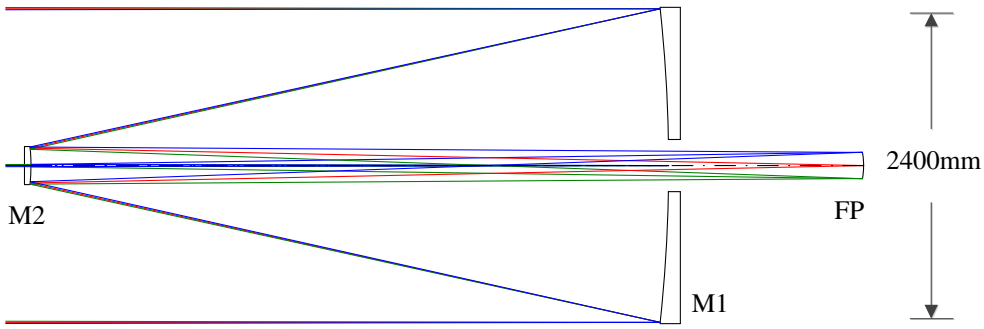

Fig. 9. Optical layout of the Hubble Space Telescope.

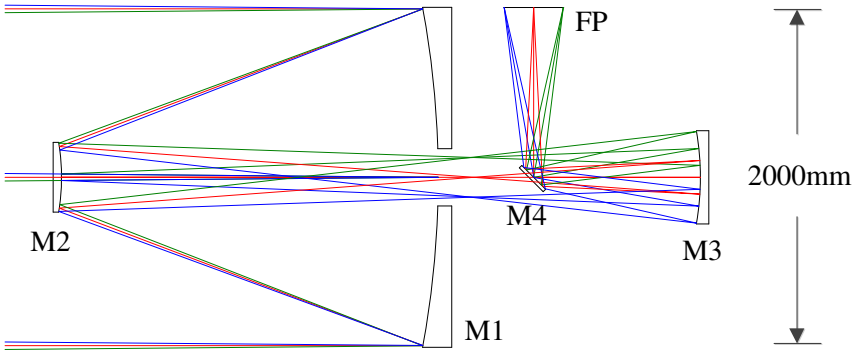

Fig. 10. Optical layout of the preliminary SNAP telescope.

In this case, the accuracy of the field diversity method within different perturbation ranges (Case 1–Case 3) and under different noise levels (Case 3–Case 5) is shown in Figs. 7(a) and 7(b), respectively. The accuracy of the defocus diversity method within different perturbation ranges (Case 1–Case 3) and under different noise levels (Case 3–Case 5) is shown in Figs. 8(a) and 8(b), respectively.

Comparing Fig. 7 with Fig. 8, we can obtain similar results with the case of the HST. Specifically, on one hand, in the noise-free cases, the accuracy of the focus diversity method is higher, which is also unaffected by the change in the perturbation range; on the other hand, the accuracy of field diversity method is less sensitive to noise, because the knowledge of the field dependencies of different aberration types that is inherent in the field diversity method can impose a constraint on the recovered aberration coefficients and reduce the effect of noise.

Besides, we can also find that the accuracy of the field diversity method in Fig. 7(a) is lower than that in Fig. 5(a). The main reason is that the field of the preliminary SNAP telescope is far larger than the HST. Those aberration contributions with a high-order field dependency that are neglected in our method also increase with field, which decrease the accuracy of our method. However, this deviation is still very small (about 10^{-3}). In the presence of noise, this deviation will be covered by the effect of noise and can no longer be recognized.

5. CONCLUSION

This paper paves a way for using intensity measurements at different field positions of one image to retrieve the wavefront aberrations of monolithic mirror space telescopes. The motivation of this work is to present great facility for wavefront sensing in space telescopes and effectively improve its efficiency. To guarantee the uniqueness of the solution, a series of intensity images with known phase diversities is usually needed in the current phase retrieval wavefront sensing methods. However, to obtain these intensity images with the deliberately added diversity phases, some additional instruments (e.g., beam splitters) or operations (e.g., adjustment of the focus) are usually needed, which can pose a challenge for wavefront sensing in space telescopes. This paper first proposes a new concept for retrieving the wavefront phase of monolithic mirror space telescopes with perturbations, where the intensity measurements with phase diversities are directly obtained from different field positions of one image, without the need for any additional instruments or operations. Then the field diversity phase retrieval algorithm is proposed to realize this multifield phase retrieval concept. This work can also greatly improve the efficiency for wavefront sensing in monolithic space telescopes. Intensity measurements at several randomly selected field positions can be used to recover the whole aberration field. Relevant simulations for different cases are performed to demonstrate the feasibility and accuracy of the proposed method.

In contrast to some other research on phase diversity phase retrieval wavefront sensing which lay emphasis on the nonlinear optimization algorithms, this paper emphasizes a new phase retrieval concept and how to realize this concept. The main problem we face is that the phase diversities between the intensity measurements at multiple field positions are unknown.

To solve this problem, we first present a deep discussion on the current phase diversity algorithm. We recognize that one key point in the current phase diversity algorithm is that there is only one set of unknown parameters that is needed to be determined, while there is usually more than one intensity measurement with phase diversity that is utilized to establish the error metric. Then we present a method of using one set of the unknown parameters to express the aberrations at different field positions based on an in-depth understanding of the aberration field characteristics induced by perturbations. On this basis, we realize the multifield phase retrieval concept.

We should point out that one of the theoretical bases of this work is that most of the net aberration contributions induced by misalignments and figure errors have a very low order of field dependency and we can neglect those contributions with a higher-order field dependency. For a small perturbation range, the accuracy of this approximation is very high. However, as the perturbation range increases, the accuracy of this approximation will decrease by some extent, especially for those systems with a relatively large field of view. On the other hand, we should also note that we mainly concentrate on the case of wavefront sensing for active optics systems in space telescopes, where the perturbation range is usually not unreasonably large. Besides, the knowledge of the field dependencies of different aberration types induced by perturbations is inherent in the field diversity method. This knowledge can put a constraint on the recovered aberration coefficients and reduce the impact of noise, especially when intensity measurements at more than two field points are used to perform this field diversity method. Therefore, the method proposed in this paper can aptly apply to the wavefront sensing in space telescopes.

The field diversity phase retrieval method presented in this paper is mainly for wavefront sensing in monolithic mirror space telescopes. In the future work, we will investigate how to extend this method to wavefront sensing in segmented mirror space telescopes.

APPENDIX A

This appendix provides the optical prescriptions and layouts for the Hubble Space Telescope and the preliminary SNAP telescope simulated in Section 4. The optical prescriptions for the Hubble Space Telescope and the preliminary SNAP telescope are presented in Tables 3 and 4, respectively. The layouts for the Hubble Space Telescope and the preliminary SNAP telescope are presented in Figs. 9 and 10, respectively.

Funding. National Natural Science Foundation of China (NSFC) (61205143).

REFERENCES

1. J. K. Davies, "Observing with the Hubble Space Telescope," Contemp. Phys. **40**, 271–274 (1999).
2. L. Noethe, "Active optics in modern, large optical telescopes," Prog. Opt. **43**, 1–69 (2001).
3. J. R. Fienup, "Phase retrieval algorithms: a comparison," Appl. Opt. **21**, 2758–2769 (1982).
4. B. H. Dean, D. L. Aronstein, J. S. Smith, R. Shiri, and D. S. Acton, "Phase retrieval algorithm for JWST flight and testbed telescope," Proc. SPIE **6265**, 626511 (2006).
5. R. W. Gerchberg and W. O. Saxton, "A practical algorithm for the determination of phase from image and diffraction plane pictures," Optik **35**, 237–246 (1972).
6. D. L. Misell, "An examination of an iterative method for the solution of the phase problem in optics and electron optics," J. Phys. D **6**, 2200–2216 (1973).
7. R. A. Gonsalves and R. C. Hidlaw, "Wavefront sensing by phase retrieval," Proc. SPIE **207**, 32–39 (1979).
8. R. A. Gonsalves, "Phase retrieval and diversity in adaptive optics," Opt. Eng. **21**, 829–832 (1982).
9. R. G. Paxman, T. J. Schulz, and J. R. Fienup, "Joint estimation of object and aberrations by using phase diversity," J. Opt. Soc. Am. A **9**, 1072–1085 (1992).
10. J. R. Fienup, "Phase-retrieval algorithms for a complicated optical system," Appl. Opt. **32**, 1737–1746 (1993).
11. R. G. Paxman and J. R. Fienup, "Optical misalignment sensing and image reconstruction using phase diversity," J. Opt. Soc. Am. A **5**, 914–923 (1988).
12. J. R. Fienup, J. C. Marron, T. J. Schulz, and J. H. Seldin, "Hubble Space Telescope characterized by using phase retrieval algorithms," Appl. Opt. **32**, 1747–1767 (1993).
13. C. Roddier and F. Roddier, "Combined approach to the Hubble Space Telescope wave-front distortion analysis," Appl. Opt. **32**, 2992–3008 (1993).
14. D. C. Redding, P. Dumont, and J. Yu, "Hubble Space Telescope prescription retrieval," Appl. Opt. **32**, 1728–1736 (1993).
15. C. Roddier and F. Roddier, "Wavefront reconstruction from defocused images and the testing of ground-based optical telescopes," J. Opt. Soc. Am. A **10**, 2277–2287 (1993).
16. D. S. Acton, P. Atcheson, M. Cermak, L. Kingsbury, F. Shi, and D. C. Redding, "James Webb Space Telescope wavefront sensing and control algorithms," Proc. SPIE **5487**, 887–896 (2004).
17. P. Bao, F. Zhang, G. Pedrini, and W. Osten, "Phase retrieval using multiple illumination wavelengths," Opt. Lett. **33**, 309–311 (2008).
18. A. Mazine and K. Heggarty, "Phase mapping and wavefront analysis based on multi-illumination light fields generated by a spatial light modulator," Appl. Opt. **50**, 2679–3691 (2011).
19. M. R. Bolcar and J. R. Fienup, "Sub-aperture piston phase diversity for segmented and multi-aperture systems," Appl. Opt. **48**, A5–A12 (2009).
20. G. R. Brady, M. Guizar-Sicairos, and J. R. Fienup, "Optical wavefront measurement using phase retrieval with transverse translation diversity," Opt. Express **17**, 624–639 (2009).
21. M. Guizar-Sicairos and J. R. Fienup, "Phase retrieval with transverse translation diversity: a nonlinear optimization approach," Opt. Express **16**, 7264–7278 (2008).
22. D. B. Moore and J. R. Fienup, "Subaperture translation estimation accuracy in transverse translation diversity phase retrieval," Appl. Opt. **55**, 2526–2536 (2016).
23. H. I. Campbell, S. Zhang, and A. H. Greenaway, "Generalized phase diversity for wave-front sensing," Opt. Lett. **29**, 2707–2709 (2004).
24. R. V. Shack and K. P. Thompson, "Influence of alignment errors of a telescope system on its aberration field," Proc. SPIE **251**, 146–153 (1979).
25. K. P. Thompson, "Aberration fields in tilted and decentered optical systems," Ph.D. dissertation (University of Arizona, 1980).
26. K. Thompson, "Description of the third-order optical aberrations of near-circular pupil optical systems without symmetry," J. Opt. Soc. Am. A **22**, 1389–1401 (2005).
27. T. Schmid, K. P. Thompson, and J. P. Rolland, "Misalignment-induced nodal aberration fields in two-mirror astronomical telescopes," Appl. Opt **49**, D131–D144 (2010).
28. K. P. Thompson, T. Schmid, and J. P. Rolland, "The misalignment induced aberrations of TMA telescopes," Opt. Express **16**, 20345–20353 (2008).
29. T. Schmid, J. P. Rolland, A. Rakich, and K. P. Thompson, "Separation of the effects of astigmatic figure error from misalignments using nodal aberration theory (NAT)," Opt. Express **18**, 17433–17447 (2010).
30. K. Fuerschbach, J. P. Rolland, and K. P. Thompson, "Extending nodal aberration theory to include mount-induced aberrations with application to freeform surfaces," Opt. Express **20**, 20139–20155 (2012).

31. K. Fuerschbach, J. P. Rolland, and K. P. Thompson, "Theory of aberration fields for general optical systems with freeform surfaces," Opt. Express **22**, 26585–26606 (2014).
32. G. Ju, C. Yan, Z. Gu, and H. Ma, "Computation of astigmatic and trefoil figure errors and misalignments for two-mirror telescopes using nodal aberration theory," Appl. Opt **55**, 3373–3386 (2016).
33. G. Ju, C. Yan, Z. Gu, and H. Ma, "Aberration fields of off-axis two-mirror astronomical telescopes induced by lateral misalignments," Opt. Express **24**, 24665–24703 (2016).
34. L. Noethe, P. Schipani, R. Holzlöhner, and A. Rakich, "A method for the use of ellipticities and spot diameters for the measurement of aberrations in wide-field telescopes," Adv. Opt. Technol. **3**, 315–333 (2014).
35. P. Schipani, L. Noethe, D. Magrin, K. Kuijken, C. Arcidiacono, J. Argomedo, M. Capaccioli, M. Dall'Ora, S. D'Orsi, J. Farinato, D. Fierro, R. Holzlöhner, L. Marty, C. Molfese, F. Perrotta, R. Ragazzoni, S. Savarese, A. Rakich, and G. Umbriaco, "Active optics system of the VLT survey telescope," Appl. Opt. **55**, 1573–1583 (2016).
36. R. Holzlöhner, A. Rakich, L. Noethe, K. Kuijken, and P. Schipani, "Fast active optics control of wide-field telescopes based on science image analysis," Proc. SPIE **9151**, 91512I (2014).
37. R. Holzlöhner, S. Taubenberger, A. P. Rakich, L. Noethe, P. Schipani, and K. Kuijken, "Focal-plane wavefront sensing for active optics in the VST based on an analytical optical aberration model," Proc. SPIE **9906**, 99066E (2016).
38. H. Mao and D. Zhao, "Alternative phase-diverse phase retrieval algorithm based on Levenberg–Marquardt nonlinear optimization," Opt. Express **17**, 4540–4552 (2009).
39. D. Yue, S. Xu, and H. Nie, "Co-phasing of the segmented mirror and image retrieval based on phase diversity using a modified algorithm," Appl. Opt **54**, 7917–7924 (2015).
40. P. G. Zhang, C. L. Yang, Z. H. Xu, Z. L. Cao, Q. Q. Mu, and L. Xuan, "Hybrid particle swarm global optimization algorithm for phase diversity phase retrieval," Opt. Express **24**, 25704–25717 (2016).
41. R. K. Tyson, "Conversion of Zernike aberration coefficients to Seidel and high-order power-series aberration coefficients," Opt. Lett. **7**, 262–264 (1982).